

Rapid Communications

The Rapid Communications section is intended for the accelerated publication of important new results. Manuscripts submitted to this section are given priority in handling in the editorial office and in production. A Rapid Communication may be no longer than 3½ printed pages and must be accompanied by an abstract and a keyword abstract. Page proofs are sent to authors, but, because of the rapid publication schedule, publication is not delayed for receipt of corrections unless requested by the author.

Bragg-case neutron interferometry

A. Zeilinger, C. G. Shull, J. Arthur, and M. A. Horne*

Department of Physics, Massachusetts Institute of Technology, Cambridge, Massachusetts 02139

(Received 28 April 1983)

The successful experimental test of a two-crystal Bragg-case neutron interferometer that is topologically equivalent to a Jamin interferometer is reported. The intensity distributions behind the interferometer are found to be in excellent agreement with those expected from dynamical diffraction theory. The distinguishing feature of this interferometer type is the absence of Borrmann spreading in one of the interfering beams. This would facilitate the use of very narrow beams in neutron interferometry.

The first and also the most commonly used type of perfect crystal interferometer^{1,2} for use with x-ray or neutron radiation is the LLL type, which employs Laue-case diffraction in three successive crystal plates. Shortly after its invention it was realized that Bragg-case diffraction could equally well be utilized in an angstrom-wave interferometer. This was demonstrated by the successful operation of a BBB interferometer with x rays.³ None of these devices make explicit use of the peculiar in-crystal propagation properties of the radiation which are predicted by the dynamical diffraction theory (e.g., the Borrmann fan spreading). However, use of those properties is essential for the operation of interferometers consisting of only two crystal plates, as has been shown by the development of the LL interferometer.⁴ An interferometer employing in-crystal propagation features in the Bragg case has been proposed by Hart⁵ in the form of a two-crystal Bragg (BB) interferometer. He realized that such an interferometer would be more useful for neutrons than for x rays due to the difference in the absorption for these two forms of radiation. This type of interferometer has also been discussed in reviews of the subject.^{6,7} It is the purpose of the present Communication to show its successful realization with thermal neutrons and to discuss some of its possible applications.

The operational principle of a Bragg-case interferometer is shown in Fig. 1. Radiation incident at a slight deviation $\Delta\theta$ from the exact Bragg angle is partly reflected at the entrance surface of the crystal and partly transmitted into the crystal. The angle Ω between the direction of propagation inside the crystal and the crystal lattice planes, which in our case were parallel to the crystal surface, is given (see, e.g., Ref. 8) by

$$\tan \Omega = \left(\frac{y^2 - 1}{y^2} \right)^{1/2} \tan \theta_B, \tag{1}$$

where

$$y = - \frac{E \Delta\theta \sin(2\theta_B) + V(0)}{[V(\vec{G})V(-\vec{G})]^{1/2}}. \tag{2}$$

E is the kinetic energy of the neutron, θ_B is the Bragg angle, $V(0)$ is the mean neutron-crystal interaction potential,

and $V(\vec{G})$ is its Fourier component appropriate for the reflection used. Equation (1) shows that radiation with $|y| < 1$ cannot propagate into the crystal. This corresponds to the 100% reflectivity region of the Darwin plateau.

Radiation which is incident outside of the Darwin region has its amplitude split into reflected and transmitted parts at the entrance surface. The reflected part, together with the radiation from within the plateau region, constitutes the beam B1. The transmitted part travels through the crystal where part of it is reflected from the back face and, following partial transmission at the original entrance face, leaves the crystal as B2 traveling exactly parallel to the partially reflected component of B1. Dynamical diffraction theory

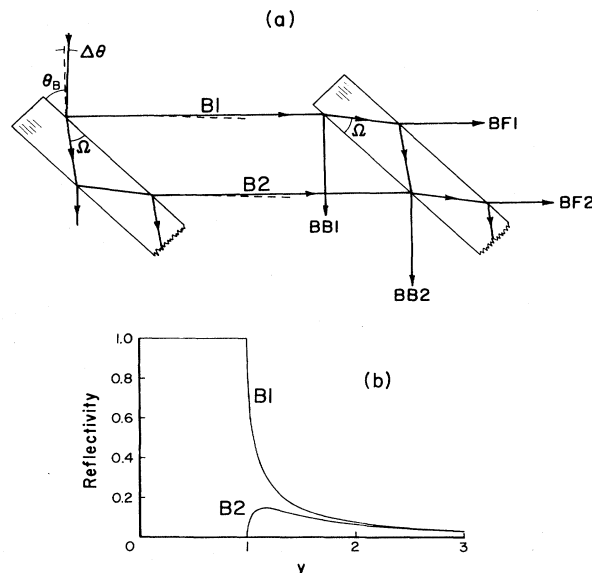


FIG. 1. Operational characteristics of the BB interferometer: (a) neutron optical beam paths and (b) reflectivity of the first crystal plate for the two interferometer beams B1 and B2.

predicts the reflectivity of these beams, defined as the ratio of their intensities to that of the original beam, to depend only upon the y value as shown in Fig. 1(b). It is to be noted that components of the B1 beam for $|y| > 1$ will be coherent with equivalent components of the B2 beam.

The second crystal plate serves to recombine these coherent components upon spatial overlapping to form phase-sensitive interference beams BB2 and separately BF2. Part of the amplitude of the B1 beam is reflected at the back face of the second crystal and is recombined upon front-face transmission with that part of the B2 beam which suffers front-face reflection thereby forming exiting beam BB2. A second exiting beam BF2 formed of mixed components also originates from the same mixing point and this can also serve as an interference beam. Figure 1(a) also illustrates that there is complete equivalence in the trajectories of the two components forming beam BB2 but not for beam BF2. This implies that higher interference contrast will be available in exiting beam BB2 when phase modification is introduced in either of beams B1 or B2.

The principle of this Bragg type of interferometer has been tested with neutrons with use of a silicon crystal which is routinely used in this laboratory as an LL interferometer.⁴ The plates of this crystal are each 9.186 mm thick and are 37.465 mm apart. These plates are cut parallel to (220) crystal planes which are used as the Bragg diffracting planes in the present study. Neutrons from the MIT reactor were first reflected from a graphite monochromator and passed through a pyrolytic graphite filter for removal of second-order wavelength contamination. A primary wavelength of 2.717 Å with a wavelength spread of ± 0.015 Å was selected, resulting in a mean Bragg angle of 45.04° at the interferometer, and the filter reduced the second-order contamination to 2% of the primary intensity. Vibration isolation of the interferometer system was accomplished by mounting it on top of a mass (25 kg of lead) supported on a small air-filled rubber tube.

The interferometer system was first tested by studying the intensity profiles of the two beams, BB1-BB2 and BF1-BF2,

released from the second crystal and passing through a scanning slit. Figure 2 shows the measured intensity distribution in the BF beam together with a first-principles dynamical diffraction theory calculation of the expected intensity allowing for the finite resolution of the measurements. In the comparison, the calculated curve has been normalized to the measured height of the A peak. Both peaks are seen to have extended shoulders on one side as is expected from the fanning effect inside the crystals according to Eq. (1). It was found from the measurements that the base intensity level between peaks A and B was higher than expected (shown in the figure), as had been noted in an earlier study.⁹ Detailed studies have shown this localized diffuse level to arise from thermal diffuse scattering in the first crystal plate.¹⁰

The intensity distribution in the BB direction given in Fig. 3 is also in excellent agreement with the dynamical diffraction theory prediction. Here again the intensity of the BB2 beam follows directly from that of the BB1 beam, whose width matches the experimental resolution. The dashed curve for the interference BB2 beam profile in Fig. 3 is that to be expected from a coherent superposition of the amplitudes for the wave components in this beam, whereas the solid curve corresponds to the incoherent sum of the intensities. It is not unexpected that the latter agrees well with observation since the measurement was performed without control of temperature stability and uniformity which affects interference action in a sensitive way.

When temperature control of the ambient crystal surroundings, on a scale of 10 mK, was introduced it was possible to sense the interference action in the BB2 beam as illustrated in Fig. 4. An aluminum phase plate of thickness 2.77 mm was used upon rotation to change the phase of the B1 beam with respect to that of the B2 beam with consequent modulation of the BB2 beam intensity. The solid curve in Fig. 4 shows the expected periodicity characteristic of the best available value of 3.449 fm for the scattering length of aluminum.¹¹

It is significant that the essential difference between this

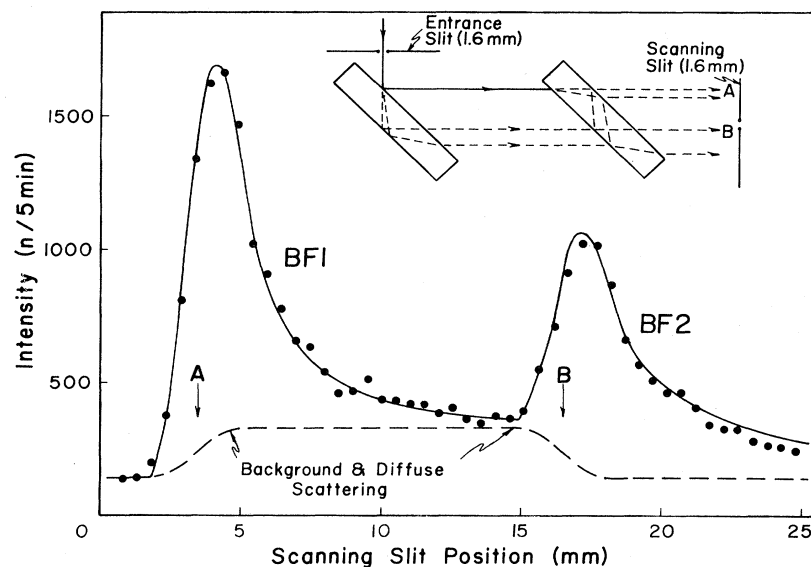


FIG. 2. Experimental result and theoretical prediction of the spatial intensity profile in the BF beam behind the interferometer.

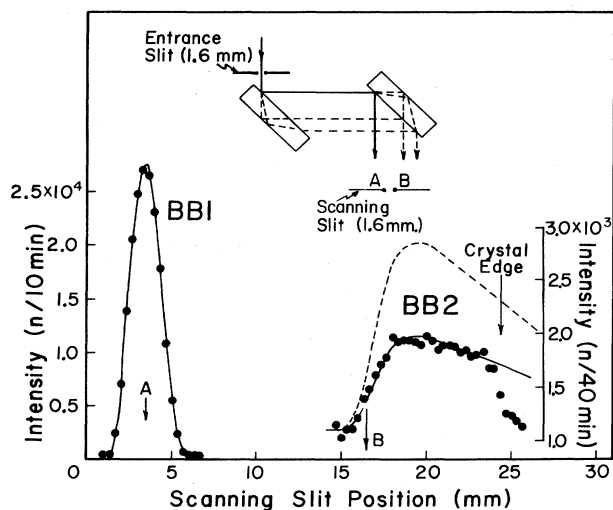


FIG. 3. Experimental result and theoretical prediction of the spatial intensity profile in the BB beam behind the interferometer.

type of neutron interferometer and other existing types is the absence of Borrmann fan spreading in one of the interfering beams (the B1 beam). This beam may be made as narrow as the incident beam collimation and primary extinction in the first crystal plate permit. This feature may be useful in applications where positional phase information from a sample is desired, or where high or very homogeneous electromagnetic fields are to be employed in an interfer-

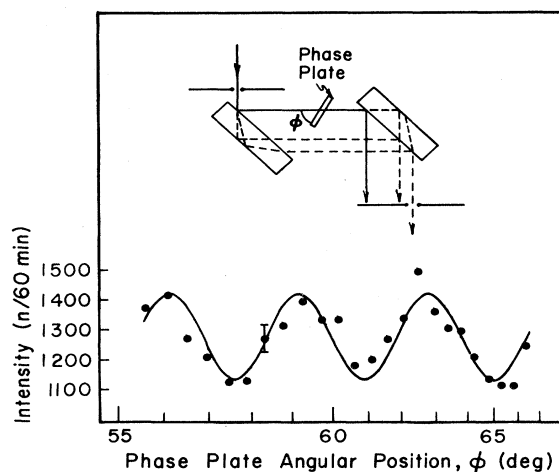


FIG. 4. Interference fringes produced by varying the optical path length through an Al phase-shifter plate.

ence experiment. From a topological point of view the present interferometer is the Bragg diffraction equivalent to the Jamin interferometer for light.¹²

We wish to acknowledge the expert fabrication of the devices used in this study by Mr. A. Daddario and the help of Mr. Daniel Gilden during the computer calculation of the intensity profiles. This work was supported by the National Science Foundation under Grant No. DMR-8021057A01.

*Permanent address: Stonehill College, North Easton, MA.

¹U. Bonse and M. Hart, *Appl. Phys. Lett.* **6**, 155 (1965).

²H. Rauch, W. Treimer, and U. Bonse, *Phys. Lett.* **47A**, 369 (1974).

³U. Bonse and M. Hart, *Z. Phys.* **194**, 1 (1966).

⁴A. Zeilinger, C. G. Shull, M. A. Horne, and G. L. Squires, in *Neutron Interferometry*, edited by U. Bonse and H. Rauch (Oxford University Press, Oxford, 1979), p. 48.

⁵M. Hart, *Rep. Prog. Phys.* **34**, 435 (1971).

⁶U. Bonse and W. Graeff, in *X-Ray Optics*, edited by H.-J. Queisser (Springer, Berlin, 1977), p. 93.

⁷W. Graeff, in Ref. 4, p. 34.

⁸H. Rauch and D. Petrascheck, in *Neutron Diffraction*, edited by H. Dachs (Springer, Berlin, 1978).

⁹C. G. Shull, *J. Appl. Crystallogr.* **6**, 257 (1973).

¹⁰A. Zeilinger and C. G. Shull, paper presented at the conference The Neutron and its Applications, Cambridge, England, 1982 (unpublished).

¹¹L. Koester and H. Rauch, *Neutron Scattering Lengths* (IAEA, Vienna, 1981).

¹²M. Born and E. Wolf, *Principles of Optics*, 6th ed. (Pergamon, Oxford, 1980), p. 310.